PTI *JOURNAL* *Technical Paper*

COMPARISON OF DIFFERENT FINITE ELEMENT METHODS ON MODELING OF POST-TENSIONED SLAB-EDGE COLUMN CONNECTIONS

BY FARSHAD JANGHORBAN AND ABDOLLAH HOSEINI

Authorized reprint from: Issue 1 2020 of the PTI *JOURNAL*

COMPARISON OF DIFFERENT FINITE ELEMENT METHODS ON MODELING OF POST-TENSIONED SLAB-EDGE COLUMN CONNECTIONS

BY FARSHAD JANGHORBAN AND ABDOLLAH HOSEINI

Recently, application of prestress techniques in concrete structures has become increasingly popular due to the possibility of reducing the slab thickness as well as the implementation of large spans. Despite the considerable advantages of prestressed concrete slabs, its behavior against lateral loads under the influence of various conditions needs to be explored. Because the verification of different parameters by experiment is costly, finite element method is an appropriate method to study the performance of these slabs and their joints with columns. In the present study, four experimental samples of unbonded post-tensioned (PT) slab-edge column connections were selected for verification by contact formulation and spring system methods. Then the aforementioned methods and their effects on the performance of the connections were considered. The results of both spring system and contact formulation methods had a good consistency in prediction of crack patterns according to the test results. Besides, due to limitations of the spring system, only the unbonded PT system can be modeled properly, whereas the contact formulation method provides the ability to model all types of PT systems.

Keywords:

bonded; contact formulation; finite element; post-tensioned; spring system; unbonded.

Introduction

Several decades have passed since the invention of prestressing techniques, but there are still no complete experiments on various parameters affecting their structural behavior. The mentioned issues reveal the need for introduction of a reliable finite element method (FEM). This method should provide the closest response to the experimental results, through which the various parameters and the validity of some of the doubtful experiments can be checked. Many efforts were made to develop finite element methods for modeling various components of post-tensioned (PT) slabs and their interaction.

Van Greunen and Scordelis (1983) explored an efficient numerical analysis procedure that can be used to predict the response of prestressed slabs. For this purpose, a computer program (NOPARC) coded in FORTRAN IV was developed. They used an updated Lagrangian formulation to evaluate the impacts of different structural geometries on the response of planar structures. To validate their method, they employed two experiments: 1) a pre-tensioned column under an eccentric load (Aroni 1968); and 2) a continuous two-way prestressed slab with unbonded tendons (Scordelis et al. 1959).

El-Mezaini and Citipitioglu (1991) demonstrated a powerful technique for the discrete representation of reinforcement in finite element analysis (FEA) of prestressed or reinforced structures. To this end, they developed an Isoperimetric element formulation with movable edge nodes. Although the presented method had successfully resulted in linear analysis, they did not consider any aspects of nonlinear performance of structures. This method provides the ability to apply different boundary conditions and use every material model.

A finite element (FE) model incorporating an arc-length solution algorithm was developed by Lou and Xiang (2006) to predict the full-range nonlinear behavior of externally prestressed concrete beams. Their model was verified with the simply supported beam specimens by Harajli et al. (1999). Also, Lou et al. (2015) developed an FE model based on the Euler-Bernoulli beam theory for the entire nonlinear analysis of bonded prestressed concrete continuous beams. To verify the proposed method, Lin (1955) and Mallick (1962) tests on bonded prestressed concrete beams were used.

Ayoub and Filippou (2010) proposed an element for the inelastic analysis of pretensioned beams. The model was based on a mixed formulation which considered deformations and forces within the element. The model was implemented in the program FEAP (Zienkiewicz and Taylor 1989) and validated with measurements from the

PTI JOURNAL, V. 16, No. 1, July 2020. Received and reviewed under Institute journal publication policies. Pertinent discussion will be published in the next issue of *PTI JOURNAL* if received within 3 months of the publication.

tests by Mitchell et al. (1993) on pretensioned concrete beams. To the authors' knowledge, no extensions of the model were reported for the simulation of pretensioned slab-column connections to date.

Huang et al. (2010) and Kang and Huang (2012) presented the spring system method to model unbonded PT structures' nonlinearity, and investigated the influence of length and number of springs on the results of this model. According to their studies, the number and length of springs did not have a significant impact on the results, and the placement of springs in proper positions could lead to convergence of results.

In Kang et al.'s (2015) paper, the contact formulation and the spring system methods were compared by using different laboratory samples, not employing the same ones. In their case, the performance of modeling methods cannot be directly compared with each other; thus, further comparison of the two methods is necessary.

Yapar et al. (2015), by validating some previous experimental works, provided a non-linear FE scheme based on bond slip failure model and plasticity damage to the pretensioned beams via simulation. Kim et al. (2017) presented an FEA approach to examine the flexural behavior of two-way PT slabs. The developed model was based on the layered and degenerated shell elements.

It is worth mentioning that many studies were performed to present FE models for characterizing the structural performance of prestressed composite beams (Saadatmanesh et al. 1989; Asta and Dezi 1998; Asta and Zona 2005; Nie et al. 2007, 2009, 2011; Hwang et al. 2015).

Research significance

In this study, four experimental tests of Sunidja et al.'s (1982) unbonded PT slab-edge column connections were verified by using spring system (Huang et al. 2010) and contact formulation (Janghorban and Hoseini 2018) methods. Then, the effect of each of the mentioned methods on the performance of the connections was evaluated.

What distinguishes this paper from Kang and Huang's 2012 PTI paper is the use of the contact formulation method to modeling four experimental samples of Foutch et al. (1990) in addition to the spring system method. The results of two modeling techniques (contact formulation and spring system) were then directly compared with each other and with the experimental results.

For this purpose, crack patterns of the top surface of specimens and the moment versus drift graph were used, which is an innovation that allows for proper comparison of the results of the two methods. In addition to the crack patterns, the moment versus drift graph presented in this article also helps to better compare the results of the two modeling methods with the laboratory results.

Numerical modeling of unbonded PT slabs

In this section, the modeling scheme of various components of the unbonded PT slab is described by contact formulation and spring system in the Abaqus Software. Abaqus is a powerful FEA software that provides complete solutions for engineering problems (Abaqus 2014).

Concrete modeling

For concrete modeling, damaged plasticity model was used. This model requires the definition of a uniaxial compressive stress-strain relationship and a tension stiffening model for concrete. The empirical stress-strain relationship by Carreira and Chu (1985) was employed to determine the uniaxial stress-strain relationship of compression, which is given in Eq. (1) to (3)

$$\frac{f_c}{f_c'} = \frac{\beta\left(\frac{\varepsilon}{\varepsilon_c'}\right)}{\beta - 1 + \left(\frac{\varepsilon}{\varepsilon_c'}\right)^{\beta}} \tag{1}$$

$$\beta = \frac{1}{1 - \left[\frac{f_c'}{\varepsilon_c' E_{it}}\right]} \tag{2}$$

$$\varepsilon_c' = (0.71 f_c' + 168) \times 10^{-5} \tag{3}$$

where f_c (MPa) is concrete compressive stress (variable); f_c'(MPa) is concrete compressive strength; ε_c' is concrete strain corresponding to f_c'; ε is concrete compressive strain corresponding to f_c (variable); and E_{it} (MPa) is initial tangent modulus of elasticity.

Huang (2012) showed that the introduction of large tension stiffening for PT structures could lead to unreasonable mesh sensitivity. Consequently, a small tension stiffening model was used in which the cracking strain was twice the corresponding strain to which f_t' is the maximum tensile stress. Other damaged plasticity model parameters were considered as default software values.

Bonded reinforcement and PT tendon modeling

In Table 1, the models used for PT tendons and bonded reinforcement were introduced. The elastic-perfectly plastic model has an acceptable accuracy to define the behavior of the reinforcing bars. To introduce the nonlinear plasticity model, the empirical stress-strain relationship proposed by Devalapura and Tadros (1992) was used, which is explained as follows

$$f_{ps} = 6.9\varepsilon_{ps}\left[A + \frac{B}{\left(1+\left(C\varepsilon_{ps}\right)^{D}\right)^{1/D}}\right] \leq 1862\text{MPa} \tag{4}$$

where f_{ps} (MPa) is stress in tendon (variable); and ε_{ps} is strain in tendon (variable). The values of A, B, C, and D in Eq. (4) are constants equal to 887, 27,613, 112.4, and 7.36, respectively.

Elements

The elements used to model various components of the unbonded PT slab-edge column connection are shown in Table 2. In exploiting the spring system, SPRINGA element with finite rotation was employed. This element is composed of the rigid link between two nodes, which can free-rotate around the nodes under large member deformations (Kang and Huang 2012). It should be noted that sheathing was used only for modeling the contact formulation scheme.

Interaction between different parts of PT slabs

This section describes how to introduce the interaction between various unbonded PT slab-edge column connection components. Simulating tendon slip is one of the hardest parts of modeling unbonded PT slabs. In the two following sections, details of the two methods were presented for unbonded system modeling.

Table 1—PT tendons and bonded reinforcement models

Part	Model
Bonded reinforcement	Elastic-perfectly plastic
PT tendons	Nonlinear plasticity

Table 2—Elements used to model various components

Part	Element
Sheathings	C3D8R
Steel plates	C3D8R
All concrete members	C3D8R
PT tendons	T3D2
Bonded reinforcement	T3D2
Springs	SPRINGA

Note: C3D8R is eight-node first-order element with reduced integration; T3D2 is two-node linear truss element.

Spring system method

Figure 1 shows how to model an unbonded PT system through a spring system. Unbonded and virtual tendons were connected by springs. The springs were considered rigid to create rotation ability and avoid bending and axial displacement. By applying a small Young's modulus, a little stiffness was given to the virtual tendons. Consequently, when these tendons were embedded in concrete, they did not have any effect on the stiffness of the slab. As a result of prestressing load balancing, load was transferred first from unbonded tendons to the virtual tendons and eventually transferred to concrete.

Contact formulation method

In the contact formulation method, the interaction between the unbonded tendon and the corresponding sheathing was introduced through the surface-to-surface capability. To provide the slip tendons in the prestressing step, the proposed relationship was considered frictionless during the entire simulation, including initial prestressing and subsequent loading. Figure 2 shows the scheme of the unbonded PT system modeling by contact formulation.

Each of the two methods used in this research has advantages and disadvantages. For example, the spring system method does not provide the ability to change tendons' boundary conditions. Moreover, modeling an unbonded PT system is possible with both methods, while bonded system is only possible through contact modeling. Therefore, the second method is more applicable although it requires more computational cost compared with the first method as it was shown by Huang (2012) and Janghorban (2017).

Embedded region constraint and MPC beam constraint

To introduce the interaction between reinforcing bars, sheathing, and virtual tendons with concrete, the embedded region constraint was used. This constraint creates a perfect bond between the concrete and the components mentioned. MPC beam constraint was also employed to model the end anchorage of the tendons. MPC beam defines a rigid beam connection to constrain the displacement and rotation of each slave node to the displacement and rotation of the control point (Janghorban et al. 2020).

Modeling prestressing procedures

Development of this study was conducted through explicit dynamic analysis. The temperature field function was used to reduce the temperature of the tendons under application of PT force.

Model verification

Four of Sunidja et al.'s test experiments of unbonded PT slab-edge column connections were selected to investigate the effect of spring system and contact formulation on joint performance. Table 3 shows the assigned symbols in this study. The symbol S was used to display the experimental samples and symbol M for displaying modeling samples. The C and S indexes represent the contact formulation and spring system models, respectively. Figure 3 illustrates one of the modeling examples.

One of the differences between the four samples tested by Sunidja et al. was the loading location, which was monotonically applied through four steel plates. Figure 4 shows the loading locations. The upper and lower ends of columns of all specimens are hinged.

In Table 4, the tendon arrangement of the samples S1, S2, S3, and S4 is shown. The reinforcing bar No. 3 with a yield stress of 73 ksi (501 MPa) and an ultimate stress of 127 ksi (874 MPa) was employed in slabs and in columns as stirrups. The reinforcing bar No. 6 with a yield stress of 73 ksi (501 MPa) and an ultimate stress of 120 ksi (830 MPa) is used in the column as longitudinal reinforcing bar. Figures 5 and 6 show the details of bonded reinforcement and tendons. Based on these two figures, the position of the reinforcing bars in all samples was the same.

All the PT tendons used in experiments were the Grade 270 seven-wire strands with a diameter of 0.37 in. (9.50 mm). To avoid bonding to the concrete, they are embedded in polyethylene sheathings with 0.50 in. (12.7 mm) diameter. Table 5 shows concrete and PT properties of experimental samples used in modeling.

A mesh sensitivity study was done for both presented methods. For this purpose, the dimensions of the mesh element were set between 0.60 and 1.7 in. (15.3 and 43.6 mm), and 1 and 4 in. (25.4 and 101.6 mm), respectively for the contact formulation method (Fig. 7), and the spring system (Fig. 8). To carry out the final analysis, the dimensions of the mesh element was chosen as 0.80 in. (20.3 mm) for the first, and different mesh dimensions (1 and 4 in. [25.4~101.6 mm]) for the second.

Figures 9 to 12 show the results of experimental samples of S1, S2, S3, and S4 with modeled samples of M1C, M1S, M2C, M2S, M3C, M3S, M4C, and M4S as moment versus drift diagrams. Analysis of the results shows that both methods

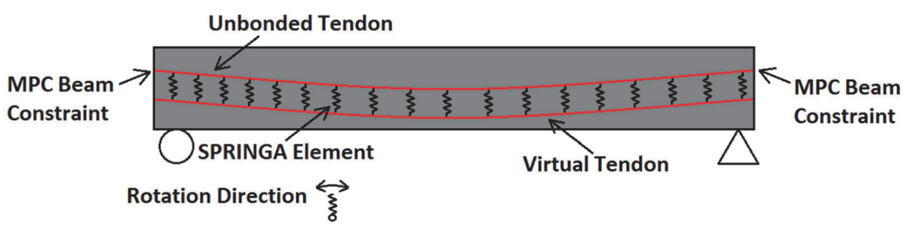

Fig. 1—Scheme of unbonded PT system modeling by using spring system (Kang and Huang 2012).

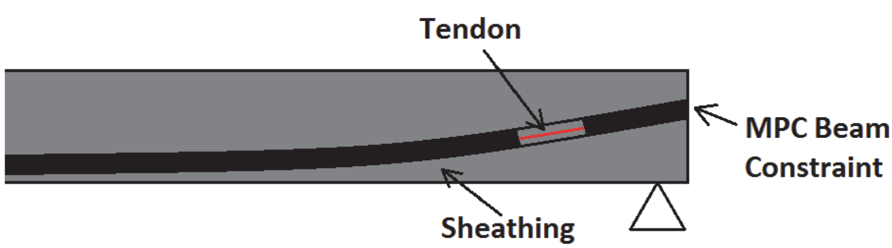

Fig. 2—Scheme of unbonded PT system modeling through contact formulation (Kang et al. 2015).

Table 3—Symbols for experimental and modeled samples

Symbol	f'_c, MPa	Modeling method	
		Spring system	Contact formulation
S1	50.37	—	—
M1S	50.37	✓	—
M1C	50.37	—	✓
S2	42.78	—	—
M2S	42.78	✓	—
M2C	42.78	—	✓
S3	42.09	—	—
M3S	42.09	✓	
M3C	42.09	—	✓
S4	48.30	—	—
M4S	48.30	✓	—
M4C	48.30	—	✓

Note: 1 MPa = 145 psi

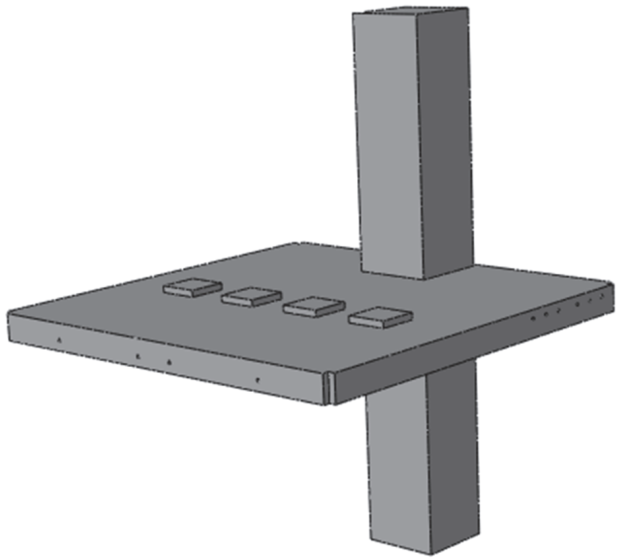

Fig. 3—One of the modeled PT slab-edge column connection samples.

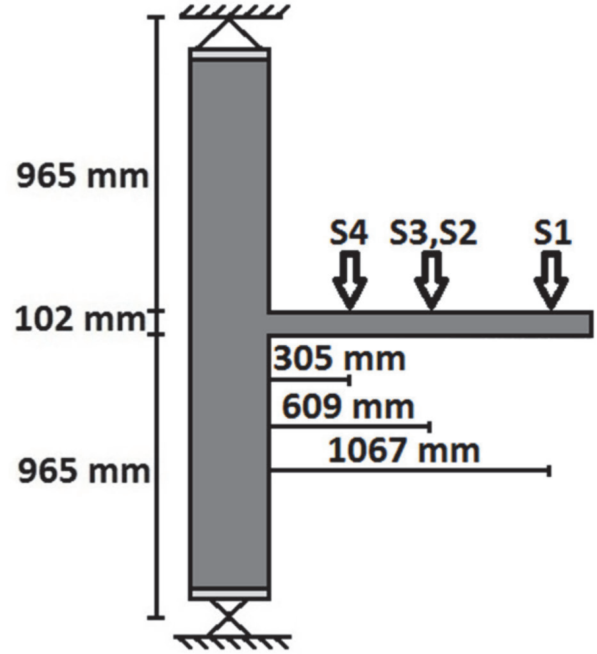

Fig. 4—Loading situations. (Note: 1 in. = 24.5 mm.)

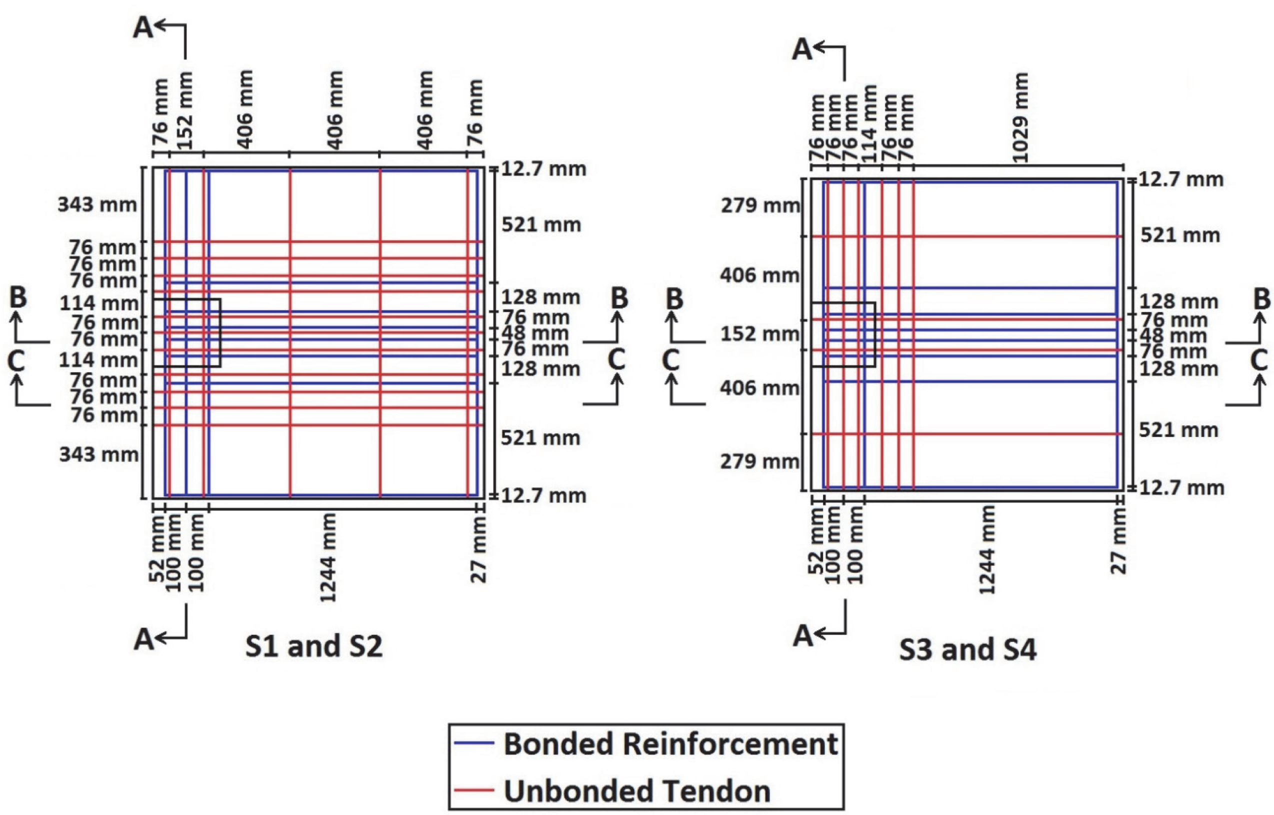

Fig. 5—Tendon arrangements and bonded reinforcement position. (Note: 1 in. = 24.5 mm.)

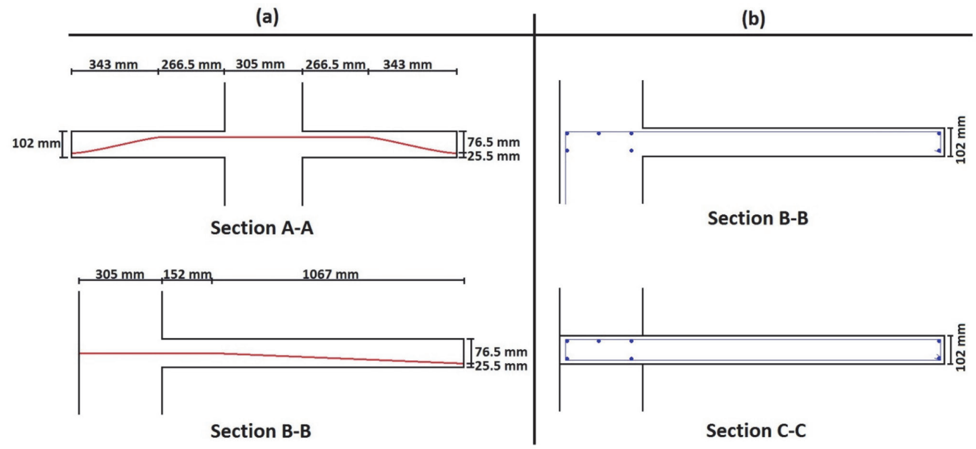

Fig. 6—(a) Tendon profile; and (b) bonded reinforcement in slab. (Note: 1 in. = 25.4 mm.)

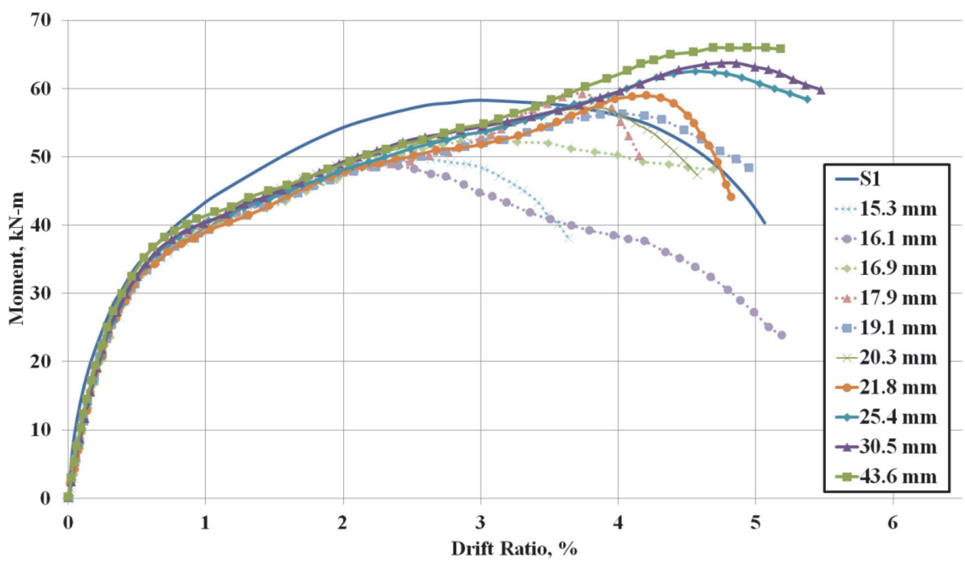

Fig. 7—Mesh study of contact formulation method (Janghorban et al. 2020). (Note: 1 in. = 25.4 mm, 1 ft-k = 1.36 kN-m)

Table 4—Tendons arrangement

Specimen	In direction of loading span	Perpendicular to direction of loading span
S1 and S2	Banded	Distributed
S3 and S4	Distributed	Banded

Table 5—Concrete and PT properties of experimental samples used in modeling

Specimen	f_c', MPa	f_r, MPa	f_{pc}, MPa		f_{pe}, MPa	
			N-S	E-W	N-S	E-W
S1	50.37	5	1.70	4.48	957.68	1150.04
S2	42.78	4.32	2.24	4.76	1265.18	1223.13
S3	42.09	4.84	2.65	1.80	1249.33	1265.18
S4	48.30	4.33	2.53	1.82	1194.17	1285.18

Note: f_c' is concrete compressive strength; f_r is modulus of rupture of concrete; f_{pc} is compressive stress in concrete; f_{pe} is effective prestress in tendon; E-W is east to west; N-S is north to south; east to west arrangement was used for loading span; 1 MPa - 145 psi.

have a good accuracy for unbonded PT slab-edge column connection modeling and have acceptable adaptation to experimental results. Although there are no significant differences in general behaviors of the two methods (Fig. 9 to 12), the results of the initial stiffness of the contact formulation method fit better with the experimental results.

Figures 13 to 16 compare the crack patterns of modeled specimens (a. contact formulation, b. spring system) with experimental specimens (c). For the contact formulation modeling, all the slabs and columns were considered (Janghorban and Hoseini 2018), whereas for the spring system, one-half of the slab and column were modeled due to its symmetry with respect to the axis perpendicular to the slab edge (Huang 2012).

Figures 13 and 15 show the flexural failure of the joint and Fig. 14 and 16 depict the punching shear failure of the connection. In Fig. 13 to 16, the failure is considered to be punching shear when the maximum plastic strains are around the column, and it is considered flexural when the maximum plastic strains are in an almost direct line in front of the column perpendicular to the loading span.

In all the aforementioned diagrams and crack patterns, there was an acceptable agreement between the results of both modelings and experiment.

Conclusions

In the current study, four test samples of unbonded PT slab-edge column connections were verified by contact formulation and spring system methods. Then, the effect of these two methods on the performance of joints was evalu-

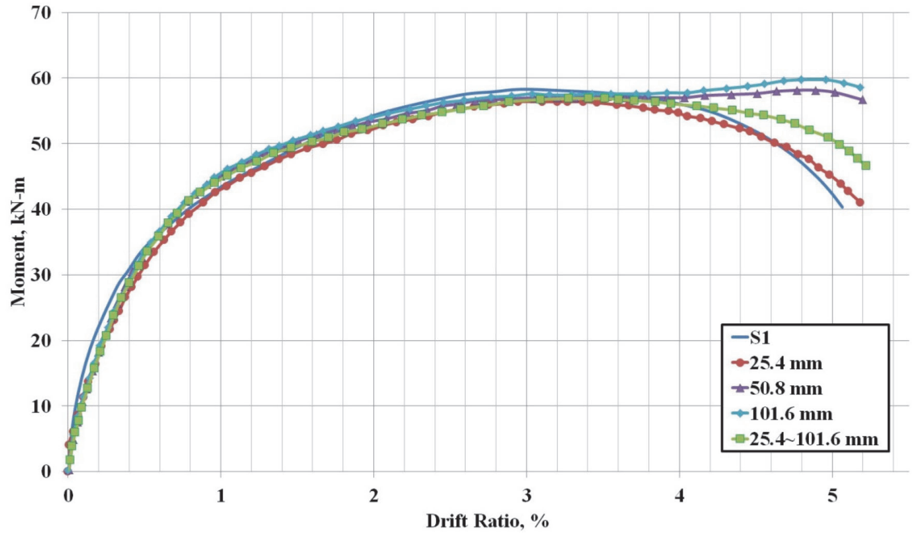

Fig. 8—Mesh study of spring system method (Huang et al. 2010). (Note: 1 in. = 25.4 mm; 1 ft-k = 1.36 kN-m.)

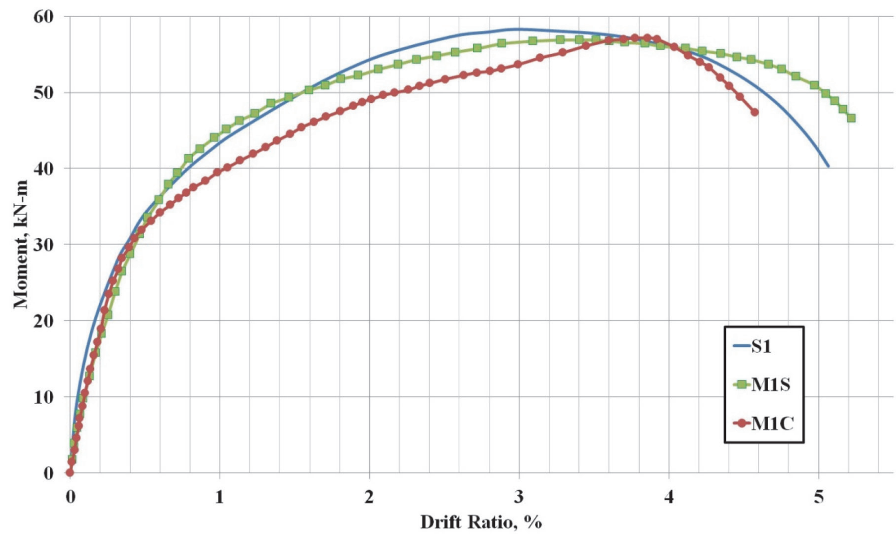

Fig. 9—Moment versus drift graph of S1, M1C, and M1S samples. (Note: 1 ft-k = 1.36 kN-m.)

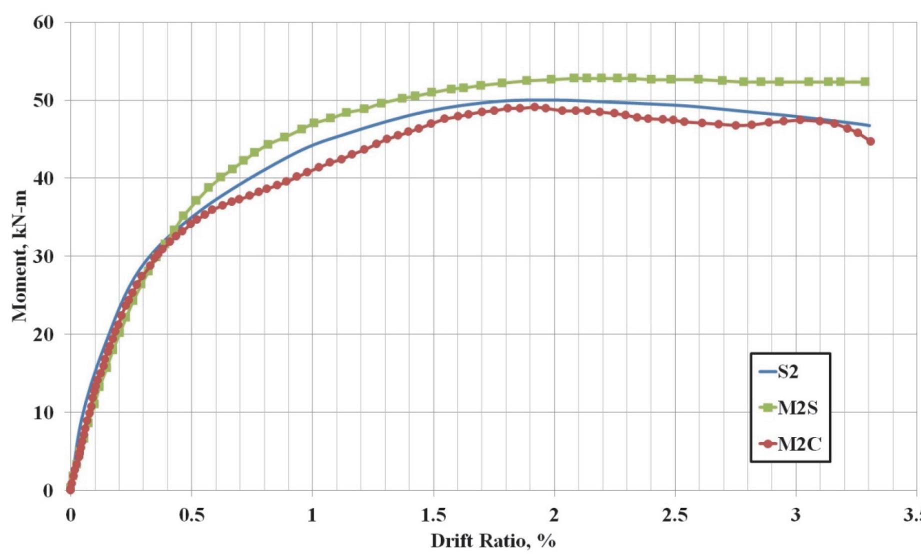

Fig. 10—Moment versus drift graph of S2, M2C, and M2S samples. (Note: 1 ft-k = 1.36 kN-m.).

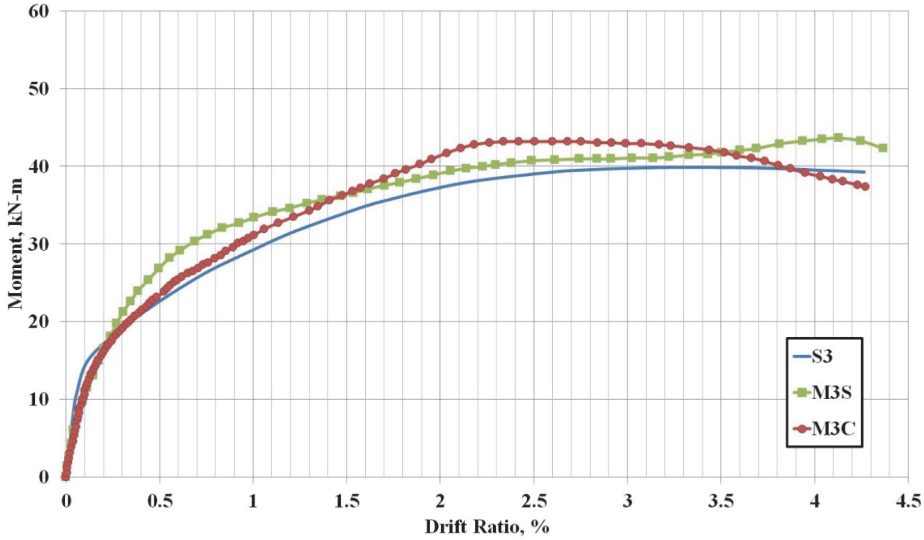

Fig. 11—Moment versus drift graph of S3, M3C, and M3S samples. (Note: 1 ft-k = 1.36 kN-m.).

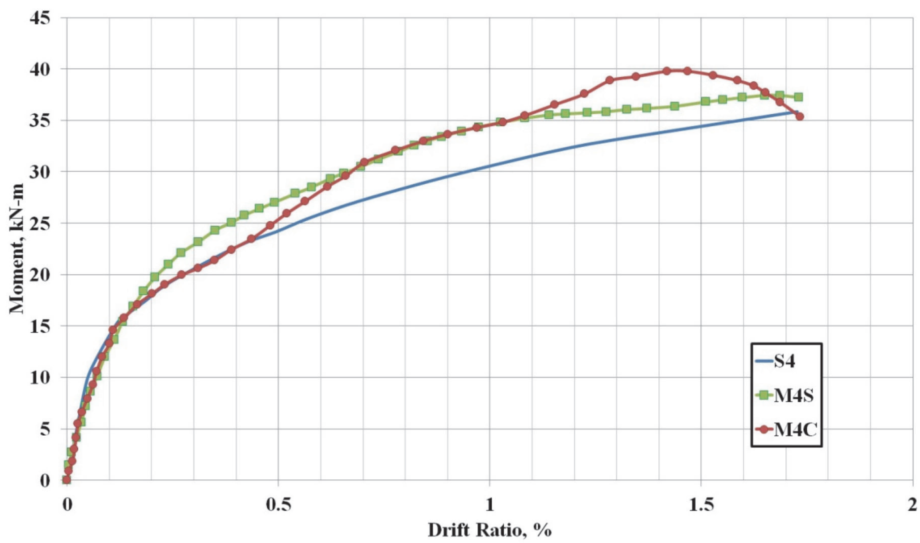

Fig. 12—Moment versus drift graph of S4, M4C, and M4S samples. (Note: 1 ft-k = 1.36 kN-m.)

ated. The following conclusions can be drawn:

1. Both the contact formulation and the spring system had the ability to predict crack patterns compared with the test results.
2. Global flexural behaviors of the two models were validated against the test results.
3. Failure types of the connections could be monitored by the mentioned methods.
4. The failure is considered to be punching shear when the maximum plastic strains are around the column, and it is considered flexural when the maximum plastic strains are in an almost direct line in front of the column perpendicular to the loading span.
5. The spring system is a simple and fast method for unbonded PT system modeling. On the other hand, the contact formulation method has more flexibility in the modeling of all types of PT systems, but it has a higher computational cost than the first method.

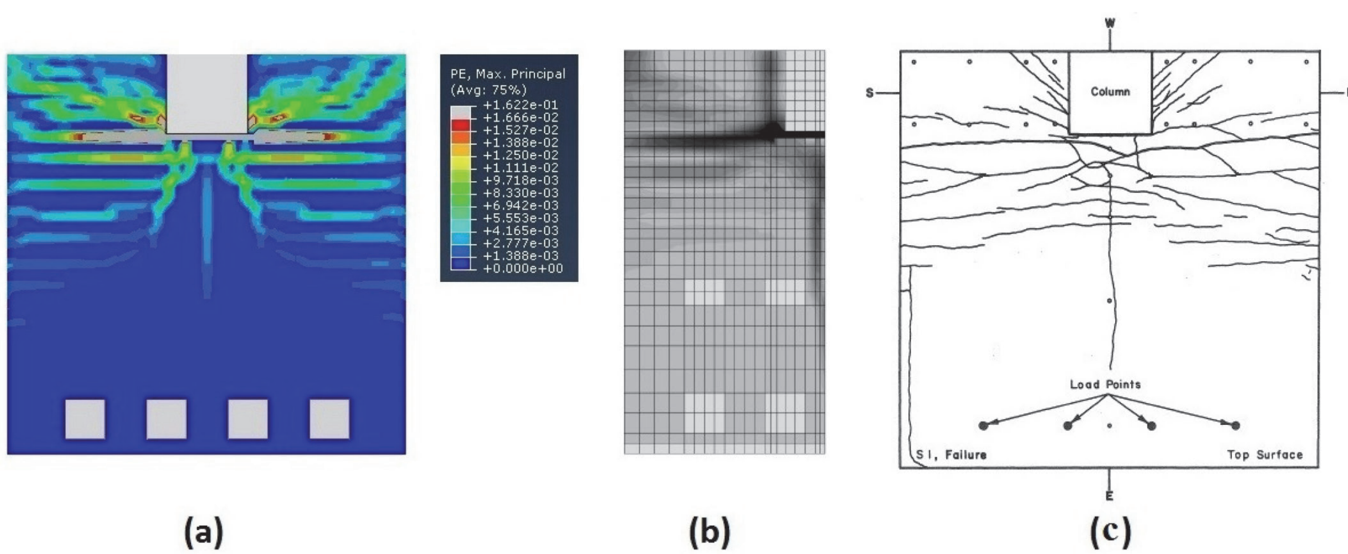

Fig. 13—Crack patterns on top surface of slabs, showing flexural failure: (a) M1C (Janghorban and Hoseini 2018); (b) M1S (Huang 2012); and (c) S1 (Sunidja et al. 1982).

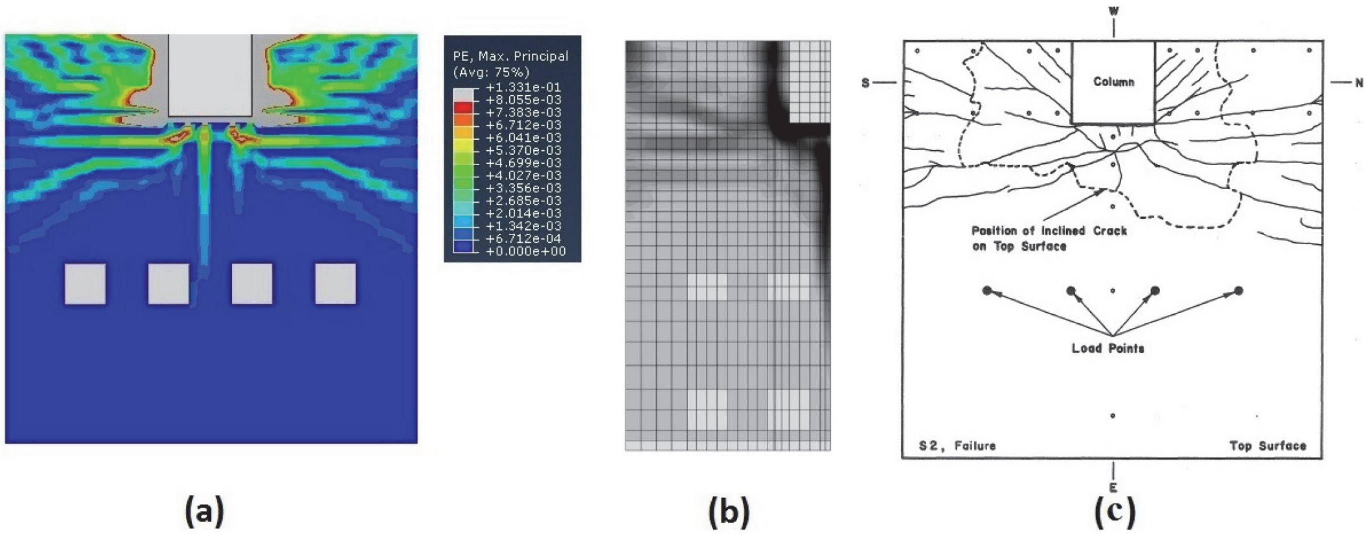

Fig. 14—Crack patterns on top surface of slabs, showing punching shear failure: (a) M2C (Janghorban and Hoseini 2018); (b) M2S (Huang 2012); and (c) S2 (Sunidja et al. 1982).

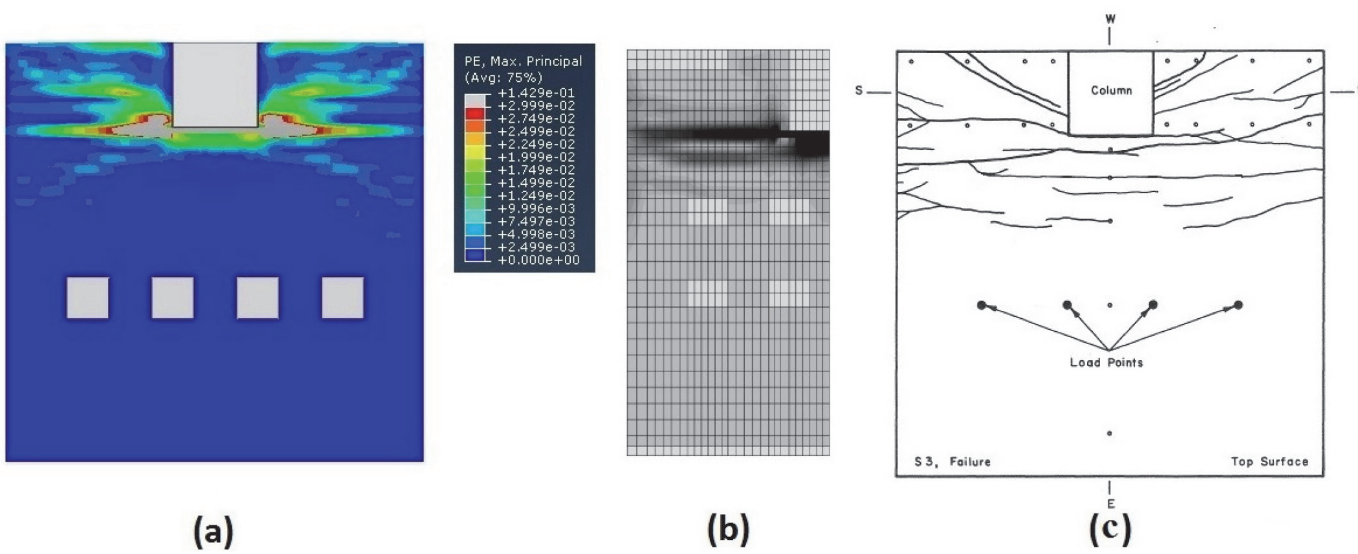

Fig. 15—Crack patterns on top surface of slabs, showing flexural failure: (a) M3C (Janghorban and Hoseini 2018); (b) M3S (Huang 2012); and (c) S3 (Sunidja et al. 1982).

References

Abaqus, 2014, "Abaqus User's Manual," Pawtucket, RI.

Aroni, S., 1968, "Slender Prestressed Concrete Columns," *Journal of the Structural Division*, ASCE, V. 94, No. 4, pp. 875-904.

Asta, A.D., and Dezi, L., 1998, "Nonlinear Behavior of Externally Prestressed Composite Beams: Analytical Model," *Journal of Structural Engineering*, ASCE, V. 124, No. 5, pp. 588-597. doi: 10.1061/(ASCE)0733-9445(1998)124:5(588)

Asta, A.D., and Zona, A., 2005, "Finite Element Model for Externally Prestressed Composite Beams with Deformable Connection," *Journal of Structural Engineering*, ASCE, V. 131, No. 5, pp. 706-714. doi: 10.1061/(ASCE)0733-9445(2005)131:5(706)

Ayoub, A., and Filippou, F.C., 2010, "Finite-Element Model for Pretensioned Prestressed Concrete Girders," *Journal of Structural Engineering*, ASCE, V. 136, No. 4, pp. 401-409. doi: 10.1061/(ASCE)ST.1943-541X.0000132

Carreira, D.J., and Chu, K.H., 1985, "Stress-Strain Relationship for Plain Concrete in Compression," *ACI Journal Proceedings*, V. 83, No. 6, pp. 797-804.

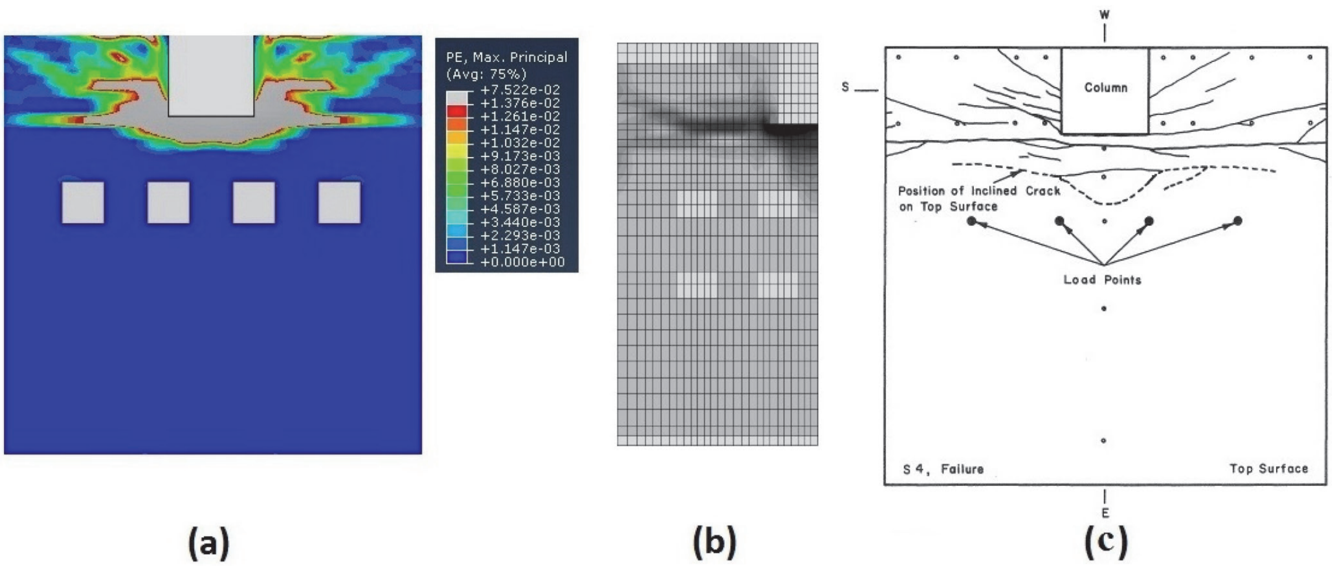

Fig. 16—Crack patterns on top surface of slabs, showing punching shear failure: (a) M4C (Janghorban and Hoseini 2018); (b) M4S (Huang 2012); and (c) S4 (Sunidja et al. 1982).

Devalapura, R.K., and Tadros, M.K., 1992, "Stress-Strain Modeling of 270 ksi Low-Relaxation Prestressing Strands," *PCI Journal*, V. 37, No. 2, pp. 100-106.

El-Mezaini, N., and Citipitioglu, E.P., 1991, "Finite Element Analysis of Prestressed and Reinforced Concrete Structures," *Journal of Structural Engineering*, ASCE, V. 117, No. 10, pp. 2851-2864. doi: 10.1061/(ASCE)0733-9445(1991)117:10(2851)

Foutch, D.A., Gamble, W.L.; and Sunidja, H., 1990, 'Tests of Post-Tensioned Concrete Slab-Edge Column Connections', *ACI Structural Journal*, Vol. 87, No. 2, Mar.-Apr., pp.167-179.

Harajli, M.; Khairallah, N.; and Nassif, H., 1999, "Externally Prestressed Members: Evaluation of Second-Order Effects," *Journal of Structural Engineering*, ASCE, V. 125, No. 10, pp. 1151-1161. doi: 10.1061/(ASCE)0733-9445(1999)125:10(1151)

Huang, Y., 2012, "Finite Element Method for Post-Tensioned Prestressed Concrete Structures," PhD thesis, University of Oklahoma, Norman, OK.

Huang, Y.; Kang, T.H.-K.; Ramseyer, C.; and Rha, C., 2010, "Background to Multi-Scale Modelling of Unbonded Post-Tensioned Concrete Structures," *International Journal of Theoretical and Applied Multiscale Mechanics*, V. 1, No. 3, pp. 219-230. doi: 10.1504/IJTAMM.2010.033601

Hwang, J.W.; Kwak, J.H.; and Kwak, H.G., 2015, "Finite-Element Model to Evaluate Nonlinear Behavior of Posttensioned Composite Beams with Partial Shear Connection," *Journal of Structural Engineering*, ASCE, V. 141, No. 8, pp. 1-15. doi: 10.1061/(ASCE)ST.1943-541X.0001174

Janghorban, F., 2017, "Assessment of Seismic Performance of Post-Tensioned Flat Slab Connections to Edge Column with Consideration of Strand Bonding Condition, Existing of Shear Cap and Concrete Compressive Strength," MSc thesis, University of Tehran Kish International Campus, Kish, Iran.

Janghorban, F., and Hoseini, A., 2018, "Numerical Assessment of Post-Tensioned Slab-Edge Column Connection Systems with and without Shear Cap," *Computers and Concrete*, V. 22, No. 1, pp. 71-81. doi: 10.12989/cac.2018.22.1.071

Janghorban, F.; Hoseini, A.; and Gamble, W.L., 2020, "Effects of Tendon Arrangements on Two-Way Unbonded Post-Tensioned Slab-Edge Column Connections," *ACI Structural Journal*, V. 117, No. 2, Mar., pp. 33-44.

Kang, T.H.-K., and Huang, Y., 2012, "Nonlinear Finite Element Analyses of Unbonded Post-Tensioned Slab-Column Connections," *PTI Journal*, V. 8, No. 1, pp. 4-19.

Kang, T.H.-K.; Huang, Y.; Shin, M.; Lee, J.D.; and Cho, A.S., 2015, "Experimental and Numerical Assessment of Bonded and Unbonded Post-Tensioned Concrete Members," *ACI Structural Journal*, V. 112, No. 6, Nov.-Dec., pp. 735-748.

Kim, M.S.; Kang, J.; and Lee, Y.H., 2017, "Analytical Model for Deflections of Bonded Posttensioned Concrete Slabs," *Advances in Materials Science and Engineering*, V. 2017, 7 pp. doi: 10.1155/2017/3037946

Lin, T.Y., 1955, "Strength of Continuous Prestressed Concrete Beams Under Static and Repeated Loads," *ACI Journal Proceedings*, V. 51, No. 6, June, pp. 1037-1059.

Lou, T., and Xiang, Y., 2006, "Finite Element Modeling of Concrete Beams Prestressed with External Tendons," *Engineering Structures*, V. 28, No. 4, pp. 1919-1926. doi: 10.1016/j.engstruct.2006.03.020

Lou, T.; Lopes, S.M.R.; and Lipes, A.V., 2015, "Numerical Modelling of Nonlinear Behaviour of Prestressed Concrete Continuous Beams," *Computers and Concrete*, V. 15, No. 3, pp. 373-389. doi: 10.12989/cac.2015.15.3.373

Mallick, S.K., 1962, "Redistribution of Moments in Two-Span Prestressed Concrete Beams," *Magazine of Concrete Research*, V. 14, No. 42, pp. 171-183. doi:10.1680/macr.1962.14.42.171

Mitchell, D.; Cook, W.D.; Khan, A.A.; and Tham, T., 1993, "Influence of High Strength Concrete on Transfer and Development Length of Pretensioning Strand," *PCI Journal*, V. 14, No. 4, pp. 62-74.

Nie, J.; Tao, M.; Cai, C.S.; and Li, S., 2011, "Analytical and Numerical Modeling of Prestressed Continuous Steel-Concrete Composite Beams," *Journal of Structural Engineering*, ASCE, V. 137, No. 12, pp. 1405-1418. doi: 10.1061/(ASCE)ST.1943-541X.0000409\

Nie, J.; Tao, M.; Cai, C.S.; and Li, S., 2009, "Deformation Analysis of Prestressed Continuous Steel-Concrete Composite Beams," *Journal of Structural Engineering*, ASCE, V. 135, No. 11, pp. 1377-1389. doi: 10.1061/(ASCE)ST.1943-541X.0000067

Nie, J.G.; Cai, C.S.; Zhou, T.R.; and Li, Y., 2007, "Experimental and Analytical Study of Prestressed Steel-Concrete Composite Beams Considering Slip Effect," *Journal of Structural Engineering*, ASCE, V. 134, No. 4, pp. 530-540. doi: 10.1061/(ASCE)0733-9445(2007)133:4(530)

Saadatmanesh, H.; Albrecht, P.; and Ayyub, B.M., 1989, "Analytical Study of Prestressed Composite Beams," *Journal of Structural Engineering*, ASCE, V. 115, No. 9, pp. 2364-2381. doi: 10.1061/(ASCE)0733-9445(1989)115:9(2364)

Scordelis, A.C.; Lin, T.Y.; and Itaya, R., 1959, "Behavior of a Continuous Slab Prestressed in Two Directions," *ACI Journal Proceedings*, V. 56, No. 6, Dec., pp. 441-460.

Sunidja, H.; Foutch, D.A.; and Gamble, W.L., 1982, "Response of Prestressed Concrete Plate-Edge Column Connections," Report No. UILU-ENG-82-2006, Structural Research Series No. 498, University of Illinois at Urbana-Champaign, Champaign, IL.

Van Greunen, J., and Scordelis, A.C., 1983, "Nonlinear Analysis of Prestressed Concrete Slabs," *Journal of Structural Engineering*, ASCE, V. 109, No. 7, pp. 1742-1760. doi: 10.1061/(ASCE)0733-9445(1983)109:7(1742)

Yapar, O.; Basu, P.K.; and Nordendale, N., 2015, "Accurate Finite Element Modeling of Pretensioned Prestressed Concrete Beams," *Engineering Structures*, V. 101, pp. 163-178. doi: 10.1016/j.engstruct.2015.07.018

Zienkiewicz, O.C., and Taylor, R.L., 1989, "The Finite Element Method: Volume 1. Basic Formulation and Linear Problems," fourth edition, McGraw-Hill, New York, NY.

Farshad Janghorban *is a Structural Engineer. He received his MS from the University of Tehran, Tehran, Iran, in 2017. His research interests include the design and analysis of reinforced and post-tensioned concrete structures.*

Abdollah Hoseini*, was an Associate Professor at the University of Tehran. His research interests included the design of reinforced and post-tensioned concrete structures. He passed away in late 2019.*